

---

---

# OPTICAL FIBER-BASED HEALTH MONITORING SYSTEM FOR BONDED STRUCTURES

Angela Trego<sup>1</sup>, Jennifer Elster<sup>2</sup>, Kay Blohowiak<sup>1</sup>, Jason Avram<sup>3</sup>, Mark Jones<sup>2</sup>

<sup>1</sup>Boeing Phantom Works

PO Box 3999, MS 84-09 Seattle WA, USA 98124-2400

<sup>2</sup>Luna Innovations

PO Box 11704 Blacksburg VA, USA 24062-1704

<sup>3</sup>Wright Patterson Air Force Base

2179 12th Street, Room 122, Wright Patterson AFB OH, USA 45433-7718

## Abstract

*Newly developed advanced aircraft structures are utilizing composite technology for improving stiffness, strength and weight properties. Such structures are commonly found in inaccessible regions where current NDE techniques are limited. Composite patch repair of cracking structure is also a newly developed technology. The development of low profile, distributed, embeddable, real-time, optical fiber sensors capable of detecting the onset of failure in aircraft structures or of adhesive bonds would eliminate a significant portion of related maintenance costs. The presented sensing system is comprised of low profile Bragg gratings for measuring load transfer and joint or composite patch failure.*

**Keywords:** Optical fiber sensors, Bragg gratings, composite patch repairs, corrosion, NDE, aging aircraft, structural health monitoring

## Introduction

In aging aircraft cracking has become a significant issue. There are several methods in use to stop and repair the cracking of the structure. One such method, the bonded repair, or “crack patching”, allows for restoration of strength and stiffness of the structure, as well as slowing crack growth by reducing the stress intensity. However, especially for critical components with bonded repairs, the crack needs to be inspected at specific intervals in order to monitor crack growth and to ensure that structural integrity is not compromised. One primary concern with repair patches, and reason for limiting use to non-load bearing aircraft parts, has been the potential degradation of load transfer capabilities due to aging and environmental effects, and that there is currently no NDI procedure for assessing bond durability [1]. To address the need for *in-situ* sensors to nondestructively monitor the health of composite patch systems and hard to inspect composite regions, optical fiber strain and chemical sensors are being developed to detect patch delamination, water penetration, and corrosive activity, as well as the load bearing capability of a composite patch repair. The sensing system is comprised of optical fiber Bragg gratings-based strain sensors. These sensors may be multiplexed with other Bragg grating-based sensors as well as long period grating-based chemical sensors [2] and embedded within the bonded joint, composite structure or

composite patch for structural health monitoring. Objectives are to detect disbands growth in the safe life zone and monitor damage growth in the parent structure. Both the Bragg and the long period grating sensor have similar signal-conditioning techniques that can be incorporated into a single monitoring system for simultaneous interrogation of multiple sensors. The following sections describe the method of operation behind the Bragg-grating strain sensor, and the proposed work plan. The development of low profile, distributed, embeddable, real-time, optical fiber sensors capable of detecting the onset of bonded joint or patch failure on repaired regions of the aircraft would eliminate a significant portion of the related maintenance costs as well as improve confidence levels in the technology, so that widespread implementation of the technology may proceed.

### Background on Sensor Design

Photo induced Bragg gratings were first demonstrated by K.O. Hill *et al.* in 1979 [3] using light from an argon-ion laser oscillating at 488 nm. Currently, the optical fiber Bragg grating is fabricated by exposing UV light through a phase mask onto the optical fiber. This fabrication process offers the capability of maintaining the pristine ultimate strength of the optical fiber by re-coating Bragg grating sensors with a protective polymer after the writing process. Inherent advantages that optical fiber Bragg grating strain sensors have over the foil strain gauge include size and flexible geometry, resistance to EMI, spark resistance, resistant to attack by most chemicals, immunity to electromagnetic interference, do not cause hazardous sparks, and allow for inexpensive distributed sensing capabilities. As opposed to the foil strain gauge, the Bragg grating strain sensor operates on self-referencing absolute measurements. This allows the user to unplug and plug into the sensor at time-based intervals without having to recalibrate. The resulting sensor element is illustrated below, in Figure 1a, along with the optical spectrum shift with strain shown in Figure 1b.

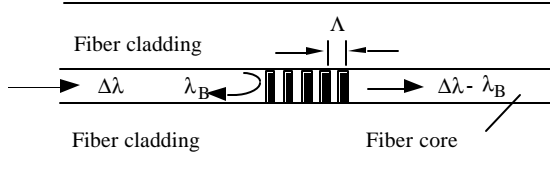


**Figure 1a. Schematic of the Bragg grating sensor illustrating refractive index variation within the core.**

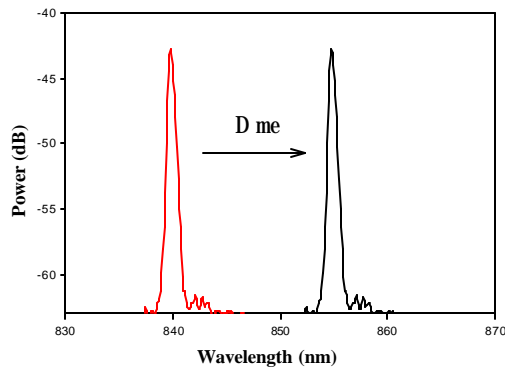


**Figure 1b. Spectrum of Bragg grating sensor , showing spectral shift with induced strain**

Here, the photo-induced planes of constant index of refraction will be oriented perpendicular to the axis of the fiber as shown in a schematic of the Bragg grating in Figure 1a. In this configuration, part of the light incident on the grating gets back reflected while most of the light will be transmitted. The reflected wavelength,  $\lambda_B$ , will interfere constructively after reflecting off each of the layers, satisfying the Bragg equation relationship:

$$\lambda_B = 2n\Lambda, \tag{1}$$

where  $n$  is the index of refraction, and  $\Lambda$  is the grating spacing. If strain is applied to the Bragg grating, the resonant reflected wavelength  $\lambda_B$  will shift by an amount given by  $\Delta\lambda_B$ , where:

$$\Delta\lambda_B/\lambda_B = (1 - P_E) \epsilon, \quad (2)$$

where  $P_E$  is the photoelastic constant for the silica fiber core. Hence by tracking  $\Delta\lambda_B$ , residual strain can be accurately monitored. Figure 1b illustrates strain measurements using the spectral shift from a Bragg grating.

For real-time data acquisition a prototype signal conditioning system with a laptop computer interface was used to interrogate the Bragg grating response by tracking the spectral shift of the reflected wavelength. Loads were applied to a beam up to 2000  $\mu\epsilon$  in compression and tension. The demonstrated Luna Prototype system can track a Bragg grating wavelength shift with a resolution of 1 picometer. This gives an estimated sensitivity of the overall system to measure strain changes on the order of 1.5  $\mu\epsilon$ .

### Testing Results

Both lapshear tests and wedge tests were conducted at the Boeing Company to demonstrate the feasibility of using Bragg gratings inside adhesive joints. The test specimen results represent behavior in adhesive joints, composite patch repairs, and composite structural areas.

#### Lapshear tests demonstrating axial strain measurements within adhesive bondlines.

Bragg grating based strain sensors that are 125 micron and 80 micron were embedded within adhesive bondlines. The following sections detail lapshear tests that are currently in progress that demonstrates the measurement of strain and load bearing capability of adhesive bondlines before and after environmental exposure in 98% RH/140 °F (60 °C) for 90 days according to Boeing Procedure #7072 Type I.

Lap shear test coupons were assembled using two 1" x 5" (2.54 cm x 3.81 cm) 2024-T3 aluminum pieces with a 1" x 1" (2.54 cm x 2.54 cm) adhesive overlap region. The two pieces of aluminum were bonded together using PAA surface preparation and FM 73 adhesive in the configuration shown in Figure 4. For each sample, an optical fiber Bragg grating strain sensor was embedded on the centerline at the adhesive/metal interface.

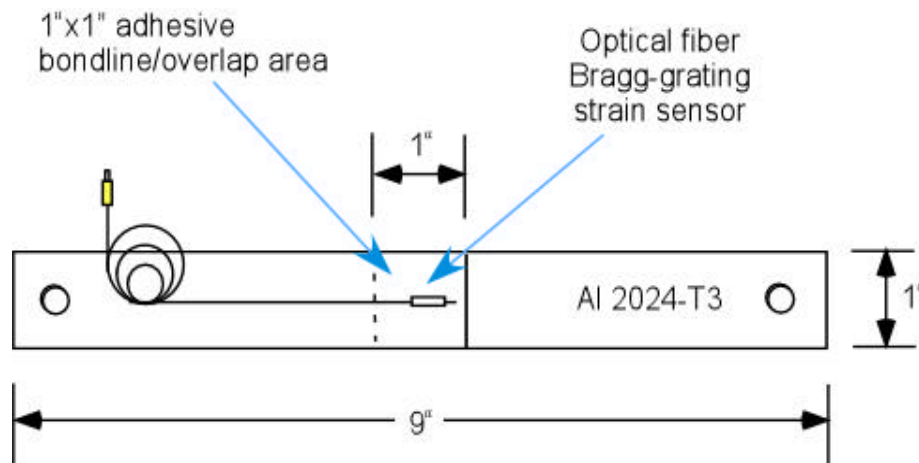
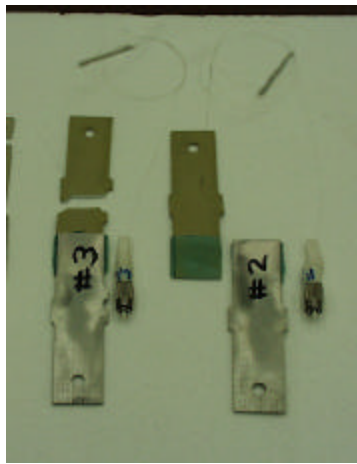


Figure 4. Schematic of lap shear coupon with embedded optical fiber Bragg grating strain sensor placed within the adhesive/metal interface.

After vacuum sealing and autoclaving, two of the test coupons were loaded under static condition until failure. Figure 5 shows a photograph of the samples after loading. As shown, test coupon #3 failed in the aluminum stem region and never failed at the adhesive bondline, and coupon #2 failed at the adhesive bondline.



**Figure 5. Unconditioned lap shear samples #2 and #3 after static loading till failure.**

Similar test coupons to those shown above were put into an environmental chamber set at 98 % RH / 140 °F (60 °C). These eight coupons will remain in the chamber for approximately 90 days, upon which they will be loaded under similar conditions (approximate test date is January 2001). From these other specimen and further testing trends will be generated.

Figure 6a below shows the load spectrum used on test coupon #3. The peak load was 3636 lbf with a 0.05"/min (1.27 cm/min) head speed. The test took a total of 2 minutes and 22 seconds until failure in the aluminum stem. This failure mechanism is indicative of the fact that the overlap region was 2" rather than 1". Figure 6b is the response from the Bragg grating during the loading of the test coupon.

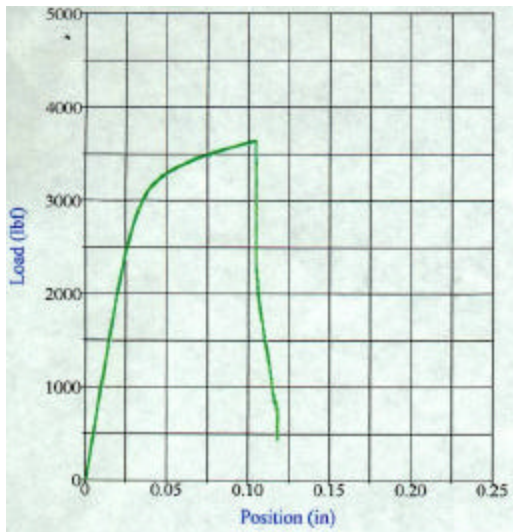


**Figure 6a. Static load spectrum for test coupon #3.**

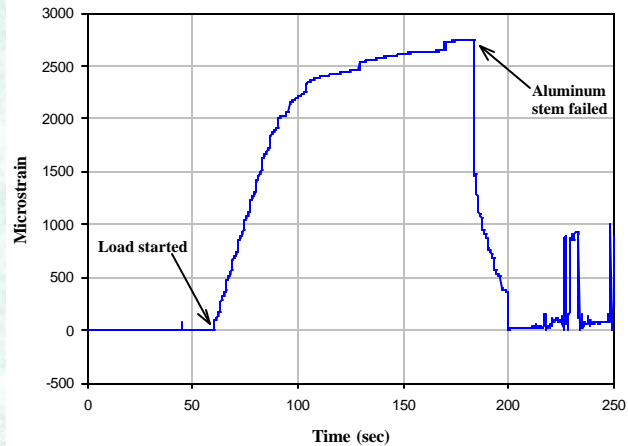


**Figure 6b. Response from Bragg strain sensor during loading of test coupon #3.**

Figure 7a below shows the load spectrum used on test coupon #2, a lap shear specimen that failed at the adhesive bondline. The peak load for this specimen was 3778 lbf with a head speed of 0.05"/min (1.27 cm/min). The test took a total of 2 minutes and 27 seconds until failure. Figure 7b is the response of the Bragg grating strain sensor during the load. This response illustrates loading of the specimen until failure at the adhesive bondline. As shown, the sensor embedded in this coupon never broke.

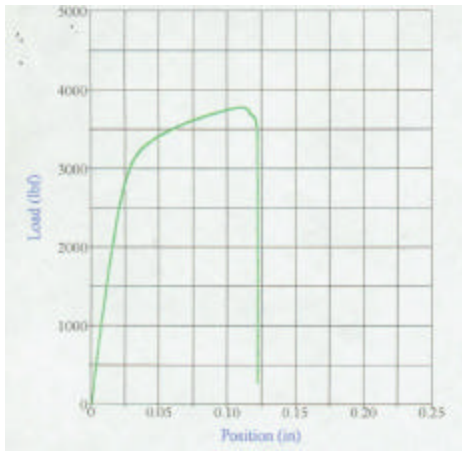


**Figure 7a. Static load spectrum for lap shear specimen #2.**

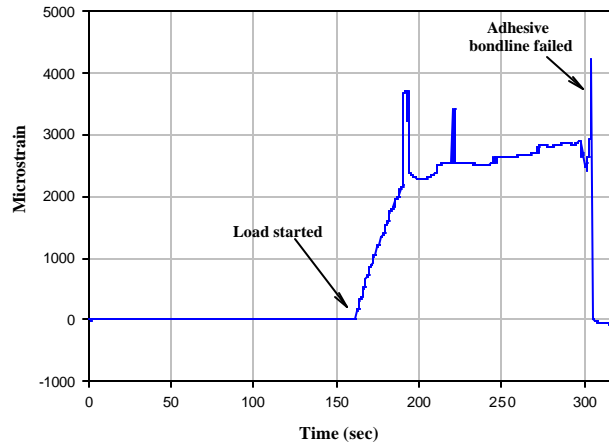


**Figure 7b. Response from Bragg strain sensor during static loading of lap shear specimen #2.**

Specimens #2 and #3 failed differently during the loading conditions. This difference in failure mechanism is illustrated in both the load spectrums shown in Figures 6a and 6b and the strain data acquired from the Bragg gratings shown in Figures 7a and 7b. The shear specimen that failed at the bondline demonstrates a curved failure line as shown in Figure 7a versus a sharp failure point demonstrated in Figure 6a. This failure mechanism is also demonstrated in Figure 7b versus 7a. As illustrated the Bragg grating strain sensor is illustrating some slipping before failure, or loss of load bearing capability. This shows up as spikes in the strain data. Future testing will further study the possible effects of slipping before failure.

**Boeing Wedge Tests demonstrating quality of surface prep and integrity of adhesive bondline.**

For the Boeing wedge tests, a matrix of 6” x 1” x 0.125” (15.24 cm x 2.54 cm x 0.318 cm) Al 2024-T3 coupons were bonded together using either the Phosphoric Acid Anodize (PAA) or the HF-Alodine surface prep and either FM73 or EA9394 adhesive according to Boeing procedure #5555. Simulated optical fiber sensors and Bragg grating strain sensors that were 80 micron and 125 micron were embedded in the wedge samples at the metal/adhesive interface. For each specimen with the real sensors, one optical fiber Bragg grating strain sensor was placed 1.1” (2.79 cm) from the end of the edge, as shown in Figure 8. The objective of this test was to determine if the optical fiber had an adverse affect on the strength of the bondline as well as to determine if the sensor could measure crack growth of the aluminum coupon. Future testing will consist of testing for trends, embedding multiplexed Bragg gratings and LPG-based moisture and corrosion sensors within the wedge samples.

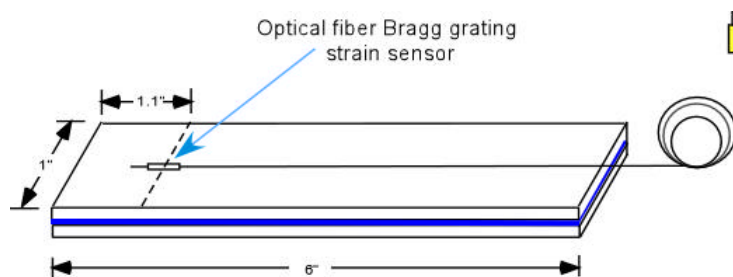


**Figure 8. Schematic of aluminum coupon with embedded optical fiber Bragg grating sensor.**

After vacuum curing, a wedge was driven into one end of the wedge coupon and the crack length (beyond the original crack length) was measured as a function of time. These wedge coupons were placed in a high humidity (100 % RH) / high temperature (140 °F/60 °C) environment. Resulting crack growths with time and failure modes were evaluated at the end of the test. Figure 9 and 10 show photographs of the wedge coupons tested at Boeing.

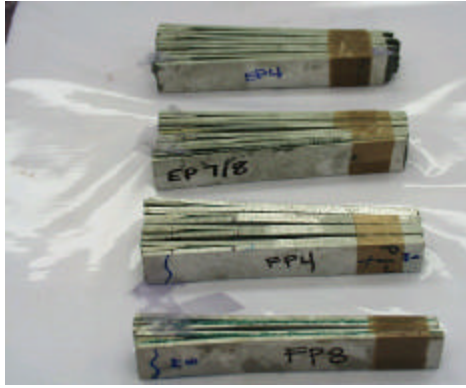


**Figure 9. Photograph of the various wedge samples with embedded optical fiber dummy sensors after 100 % RH / 140 °F exposure for 24 hrs.**



**Figure 10. Photograph of the various wedge samples with embedded optical fiber Bragg sensors after 100 % RH / 140 °F exposure for 24 hrs.**

Figure 11 shows a graph of several of the wedge coupons, with an EA9394 adhesive and a PAA surface preparation, after 24 hrs of 100 % RH / 140 °F (60 °C) exposure that have 80 micron and 125 micron optical fiber Bragg strain sensors embedded in them. Data acquired from these sensors indicate the majority of the strain was realized as the wedge was driven into the samples. Initial results indicate that further development and usage of the less obtrusive 80 micron optical fiber will be beneficial for bondline embedment applications to reduce strength and load effects from the fiber optic. These tests will be repeated using the knowledge gained in these initial experiments. Multiplexed Bragg grating strain sensors will be placed farther along the wedge crack in order to gain more data in the later stages of the crack growth. Future experiments will include multiplexing strain Bragg grating sensors with LPG-based corrosion sensors for both strain and environmental measurements.

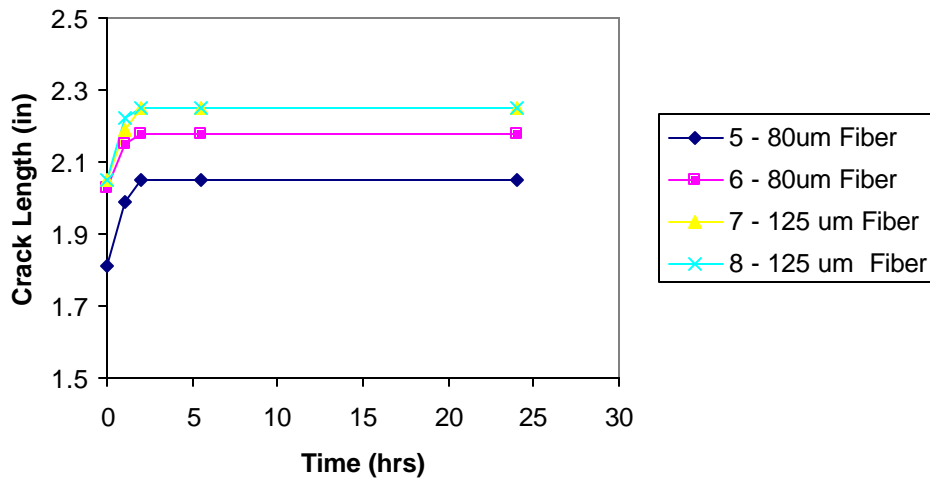


**Figure 11. Comparison of Optical Fiber Diameter for a Wedge Test.**

The inherent advantages of optical fiber-based sensors and their ability to withstand the high temperature and pressure during autoclaving were demonstrated during both the lapshear tests and the wedge tests. These advantages over other electrical based instrumentation offer the capability for future *in-situ* measurement for health monitoring applications.

## Conclusion

In conclusion, it was shown through the outlined tests the optical fiber-based sensors show promising results as an answer to monitor the health of bonded structures or composite patches. By continuing the development of these sensors, including the addition of moisture sensors and multiplexing capabilities one will be able to accurately monitor the health of composite patches and adhesive joints. The development of low profile, distributed, embeddable, real-time, optical fiber sensors capable of detecting the onset of patch failure on repaired regions of the aircraft would eliminate a significant portion of the related maintenance costs as well as improve confidence levels in the technology, so that widespread implementation of the technology may proceed.

Numerous Bragg grating strain sensors can be fabricated on the same optical fiber and designed to measure load transfer, composite delamination, and residual strain in patches used to repair cracks that occur in aging aircraft. By multiplexing the Bragg grating strain sensor with LPG-based chemical sensors, moisture as well as corrosive activity can be measured [4, 5].

The demonstrated system is built upon absolute measurements, therefore enabling the operator flexibility in monitoring the part. The user can use the system for real-time measurements by leaving the sensors connected to the signal-conditioning system or leave the sensors embedded to the structure and plug in at time-based intervals to determine health status. Such a system can be utilized for design, modeling, and validation of composite patch repairs and would ultimately allow the operator to move away from current costly time-based maintenance procedures toward health condition monitoring of bonded repairs and repaired structure.

## References

1. Baker A., On the Certification of Bonded Composite Repairs to Primary Aircraft Structures, Proceedings of, ICCM-11, Gold Coast, Australia, July 1997.
  2. Vengsarkar, A. M., P. J. Lemaire, J. B. Judkins, V. Bhatia, J. E. Sipe, and T. E. Ergodan, "Long-period fiber gratings as band-rejection filters," *Journal of Lightwave Technology*, vol. 14, 58, 1996.
  3. Hill, K. O., Y. Fujii, D. C. Johnson, and B. S. Kawasaki, "Photosensitivity in optical fiber waveguides: application to reflection filter fabrication," *Appl. Phys. Lett.*, vol. 32, no. 10, pp. 647-649, 1978.
  4. Elster, J, Greene, J, Jones, M., "Optical Fiber-Based Corrosion Sensors for Aging Aircraft, DoD/FAA/NASA Conference on Aging Aircraft, Williamsburg, VA, July 1998.
  5. Elster, J., Trego, A., Jones, M., Tulou, P., FitzPatrick, B., Perez, I.; "Corrosion Monitoring in Aging Aircraft Using Optical Fiber-Based Chemical Sensors", DoD/FAA/NASA Conference on Aging Aircraft, St Louis, MO, May 2000.
-